Received: 4 October 2021 | Revised: 28 July 2022 | Accepted: 4 August 2022

DOI: 10.1002/dep2.205

The Depositional Record
Open Access
A journal of the International Association of Sedimentologists
WILEY

ORIGINAL ARTICLE

The sedimentological death mask of a dying glacier

Daniel Paul Le Heron | **Christoph Kettler** | **Arian Wawra** | **Martin Schöpfer** | **Bernhard Grasemann**

Department of Geology, University of Vienna, Vienna, Austria

Correspondence
Daniel Paul Le Heron, Department of Geology, Josef-Holaubek-Platz 2, 1090 University of Vienna, Vienna, Austria.
Email: daniel.le-heron@univie.ac.at

Abstract

The Pasterze is Austria's largest glacier, and it is experiencing rapid downwasting and retreat. A mosaic of complex sedimentary deposits has been produced in recent years which have not hitherto been studied, yet provide excellent lessons into the facies distribution expected from a dying valley glacier. In this paper, a new glaciological–geomorphological–geological map is presented for the glacier in July 2021. Freshly exposed (since 2018) tills and flutes constitute a subglacial sediment–landform assemblage. An ice-marginal sediment–landform assemblage comprises meltwater streams, a delta system and proglacial lake terrace deposits. The supraglacial assemblage, meanwhile, includes fossil englacial channel deposits revealed by ablation, together with debris bands, rockfall deposits and supraglacial channel deposits. Collectively, these sediment–landform assemblages constitute the building blocks of a dying glacier landsystem.

KEYWORDS

glacier, lake, moraine, till, UAV

1 | INTRODUCTION AND PREVIOUS WORK

The Pasterze Glacier, in the Großglockner range, is Austria's largest glacier and since the 1852–1856 maximum has attracted detailed geomorphological (Avian et al., 2018; Kellerer-Pirklbauer et al., 2021) and structural glaciological investigations (Kellerer-Pirklbauer & Kulmer, 2019). Its recession has been extensively documented by photographs that remind us of glacier recession in a greenhouse world (Lieb, 2004). However, in the context of accelerating mass loss globally (Hugonnet et al., 2021), and amongst predictions that two thirds of glacial ice in the European Alps will have disappeared by 2100 (Zekollari et al., 2019), efforts to understand the dynamics, melt behaviour and sedimentation of valley glaciers such as the Pasterze must be intensified, integrating approaches from geology as well as geomorphology. For humanity, the demise of temperate valley glaciers has implications through the loss of storage towers providing water to communities further down-valley (Immerzeel et al., 2020), or the looming hazard of detached or collapsed glacier margins initiating catastrophic floods (Veh et al., 2020).

Historically, much effort on the Pasterze Glacier has focussed on its changing volume and area (Gspuring et al., 2004; Paschinger, 1953; Patzelt & Slupetzky, 1970; Seeland, 1883; Wakonigg, 1993; Wakonigg & Lieb, 1996), the geomorphology of its forefield (Kellerer-Pirklbauer, 2008; Kellerer-Pirklbauer et al., 2021) or structural glaciology (Herbst & Neubauer, 2000; Kellerer-Pirklbauer & Kulmer, 2019). The role of dead ice in influencing the architecture of the glacier forefield has long been known

(Lagally, 1932), and its presence has more recently been demonstrated in the 2016 forefield via electrical resistivity tomography (Seier et al., 2017). To date, sedimentological investigation has been rather limited, with the exception being detailed descriptions of sedimentary structures and processes at the 1991 ice margin in which the role of melting dead ice blocks was recognised (Krainer & Poscher, 1992). Since that time, modern sedimentological work on the Pasterze has focussed on the thickness, temporal evolution and textural characteristics of supraglacial debris with maps of debris on the surface from 1964 to 2008 (Kellerer-Pirklbauer, 2008). Otherwise, in spite of the tradition of work on this glacier, a detailed treatment of the sedimentary deposits is long overdue.

Based on terrestrial laser scanning data, Avian et al. (2018) produced a series of maps showing the geomorphological evolution of the glacier margin from 2010 to 2013. In that paper, both depositional and erosional process domains were identified in the glacier foreland land system, and particular emphasis was made on quantifying the geometry (area, percentage of total area) of the constituent landforms. Depositional process domains were split into drift-mantled slopes, dead ice bodies mantled by sediment, ice-cored terraces and their slopes and a sandur/proglacial outwash plain. Erosional process domains included glacially eroded bedrock, ice-marginal channels (some with an original subglacial origin) and gullies in drift-mantled slopes. This paper thus represented major progress in understanding the spatial relationship between landform types, and the sequential series of four maps, which showed that landforms changed on an annual basis as the result of melting dead ice bodies. Subsequently, Kellerer-Pirklbauer et al. (2021) demonstrated that an ice-proximal lake ('sandur lake' of Avian et al., 2018) was carpeted with ice at the lake bottom, with buoyant calving of the submerged ice margin bringing icebergs to the surface. The sedimentological consequences of this process merit investigation. Thus, the aims of this paper are therefore (i) to provide a new glaciological–geomorphological–sedimentological map of the glacier in July 2021, and (ii) to describe and interpret the sediment–landform assemblages at the ice terminus with particular focus on their sedimentological development.

2 | METHODOLOGY

Fieldwork was undertaken in July 2018 and July and August 2021. The first phase of fieldwork concentrated on ground-level observations, whereas the second concentrated on aerial photography with ground-level observations as control. Fieldwork comprised sedimentological and geomorphological description including sedimentary logging. Aerial photographs were collected on 12 July, 2021 using a DJI Mavic Mini drone above the glacier, allowing an area of approximately 2 km^2 to be surveyed. Individual photographs have a resolution of 4000 × 3000 pixels, and were taken with a focal length of 4.49. Using Agisoft Metashape version 1.6.3, 913 photographs were aligned, a dense point cloud generated, and both a digital elevation model (DEM, resolution 9.65 cm) and orthomosaic were produced. Following the methodology of Le Heron et al. (2019), these DEM and orthomosaic data were imported to QGIS 3.12. The orthomosaic was made semi-transparent, layered on top of the DEM, and a 'multiply' blending mode algorithm applied, with 20% brightness and 20% contrast additionally applied. Graticules were added and the data were then imported to Adobe Illustrator CC 2018 for glaciological–geomorphological–sedimentological mapping. Owing to the nature of the study, a first order characterisation of the sediment–landform assemblages, the typical sensitivity tests applied to drone-generated data (Chandler et al., 2018) were judged not to be necessary.

3 | RESULTS

3.1 | Geological setting, glaciological setting and glacier structure

Geologically, the Pasterze Glacier sits within a deeply carved valley comprising a suite of metamorphic rocks, specifically an ophiolite suite of the Bündnerschiefergruppe (Cornelius & Clar, 1935). Two principal lithologies occur, namely (i) prasinites (retrograde metabasaltic rocks mostly consisting of albite, actinolite, epidote and chlorite) and (ii) calc–mica schist. The latter expresses a well-developed foliation on the northern side of the glaciated valley, striking parallel to the valley walls. The head of the glacier is the Johannisberg (3454 m), whereas the snout lies at approximately 2100 m elevation.

In the following, a very simple overview of glacier surface structure is provided in terms of its influence on sediment–landform generation and as a repository for supraglacial sediment. Detailed structural glaciological analyses of the Pasterze Glacier, which are the subject of recently completed (Mayrhofer et al., 2022) and ongoing study, are beyond the scope of the present paper. Each of the following features can be observed on the geomorphological–sedimentological map shown in Figure 1. In summary, the glacier is characterised by a prominent longitudinal (flow parallel) foliation, expressed in terms of alternating debris-rich and debris-poor bands. At a high angle to these foliations, flow-transverse ogives are also recognised, originating from the ice fall at the

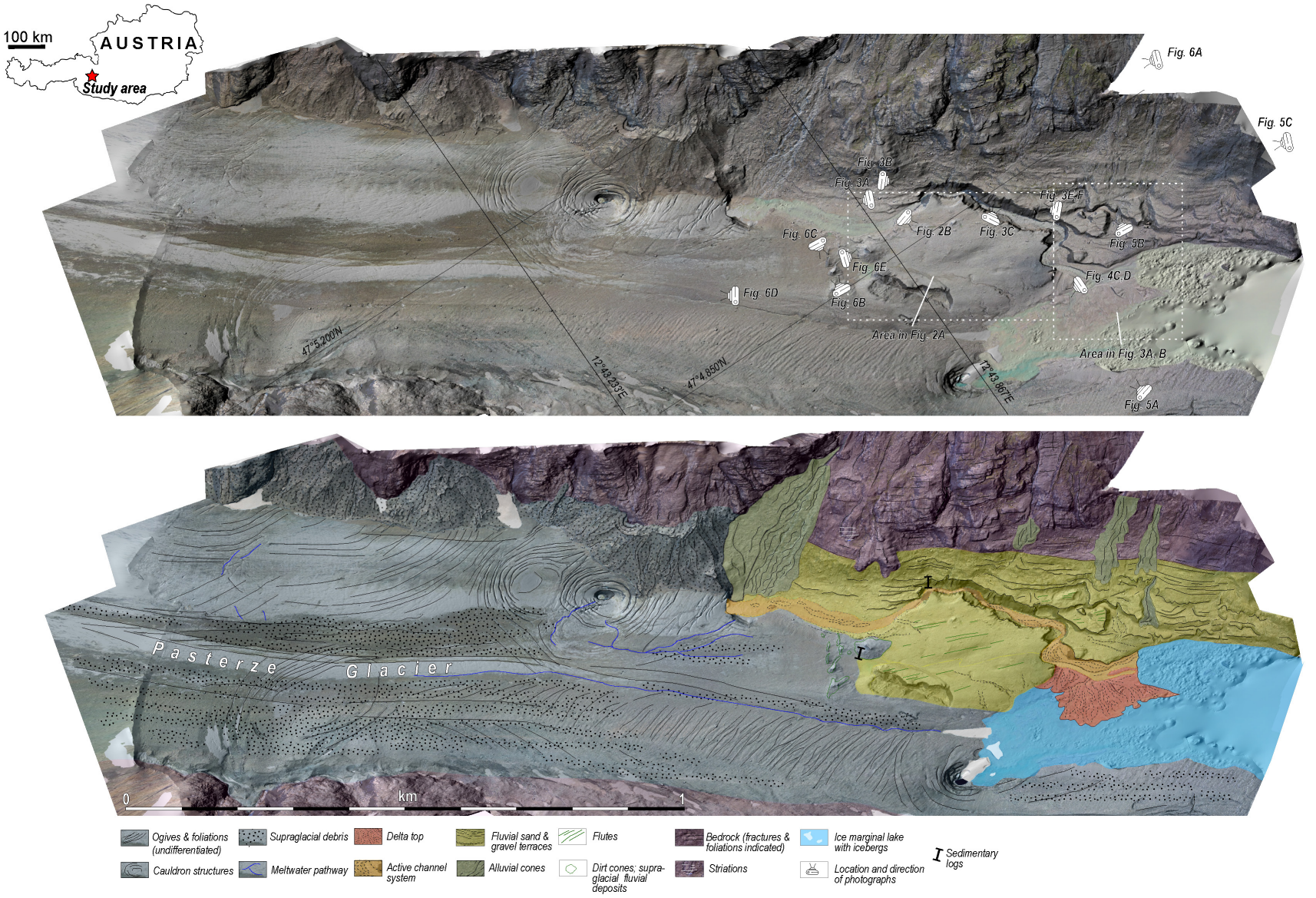

FIGURE 1 Uncrewed aerial vehicle (UAV) data and sediment landform assemblage-glaciological map of the Pasterze Glacier on 12 July 2021. The UAV data at the top of the image comprise a semi-transparent orthomosaic superimposed upon a digital elevation model following the methodology of Le Heron et al. (2019). Small camera symbols signify the direction from which photographs were taken, with the figure numbers in this paper indicated. The position of sedimentary logs is also shown on the map.

north-west flank of the glacial basin. Supraglacial meltwater streams flow parallel to longitudinal foliation, disappearing locally into moulins. Five large 'cauldron structures' cross cut the glacier surface. These consist of concentric arrangements of crevasses, with a moulin at the centre. Neighbouring cauldron structures show complex 'interference patterns' of crevasses. Finally, significant regions of the northern valley side, together with the present day snout zone, are characterised by zones of dead ice that are separated from the main body of the glacier and covered in thick supraglacial and slope-derived debris. In summary, the surface structure of the glacier provides context within which the sediment–landform assemblages can be understood. With particular emphasis on sedimentological processes and deposits, the present day (2021) ice-marginal area can be split into three distinct sediment–landform assemblages, namely (i) a subglacial assemblage, (ii) an ice-marginal fluvial and deltaic assemblage and (iii) a supraglacial assemblage. In the following, each of these are described in turn, before interpretations are offered.

3.2 | Subglacial assemblage: Description

The subglacial assemblage comprises a series of features superimposed onto underlying sands and gravels on the forefield, and represent a suite of structures developed under the glacier and now exposed by its retreat. A suite of glacial lineations cluster immediately in front of the ice margin (Figure 1); higher magnification of the drone data demonstrates that the glacial lineations are characterised by high length to width aspect ratios (>10:1) (Figure 2A). In the field, these are demonstrated to be flutes (Figure 2B) composed of sand and gravel-sized sediments whose amplitude reaches a maximum of 50 cm, and whose length

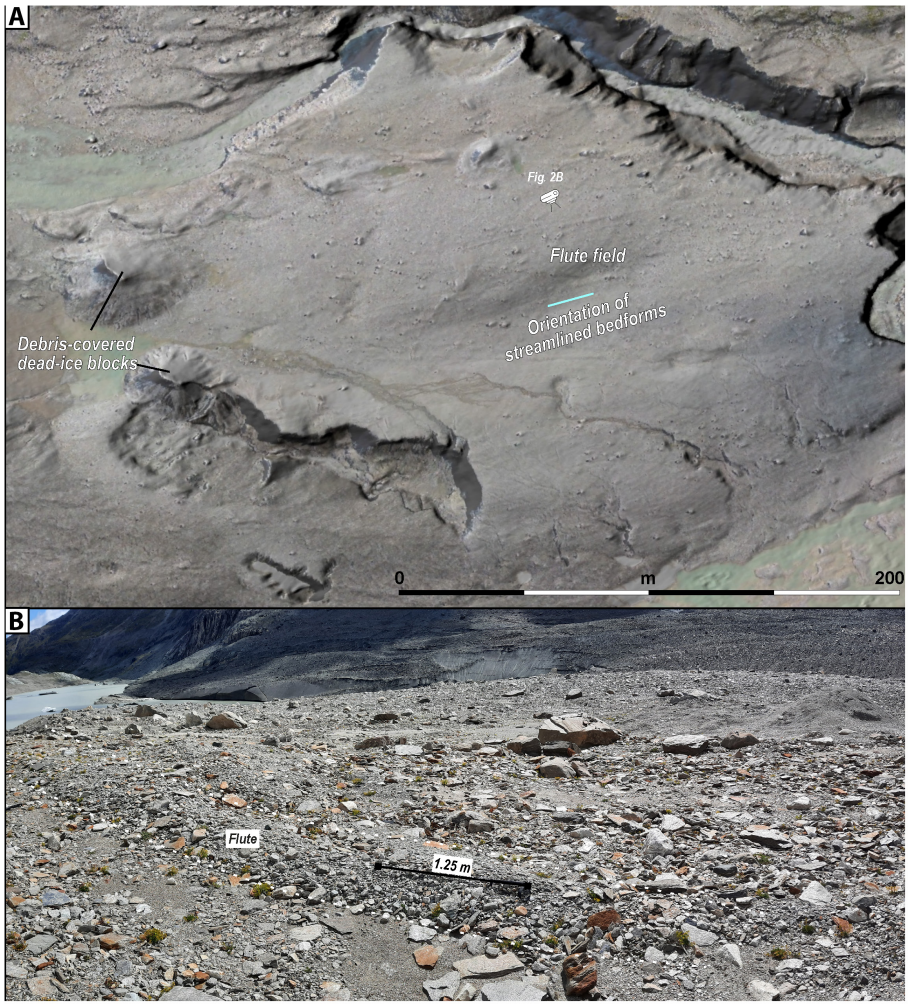

FIGURE 2 The subglacial sediment–landform assemblage. (A) An interpreted flute field exposed since 2018, immediately downstream of debris-covered dead-ice blocks. The location of the image is shown on Figure 1. The image comprises a semi-transparent orthophotograph layered over a digital elevation model. (B) Field view of the region shown in (A), with a well-preserved flute in the foreground (photograph from August, 2021).

reaches several tens of metres. These structures are locally dissected by a series of gullies. In 2018, most of the region shown in Figure 2A occupied an ice-marginal, subglacial position. The features were visible in 2021 after the region had become exposed by ice-margin recession. Flutes are also clustered on the northern side of the meltwater river, where they mantle river terrace deposits (Figure 1). In plan view, swarms of flutes are recognised, orientated slightly oblique to the longitudinal foliation in the proximal glacier (Figure 1).

3.3 | Subglacial assemblage: Interpretation

Flutes are clearly present in some Alpine valley glacier forefields (e.g. Oberseegletscher in Switzerland, Kronig et al., 2018; Gepatschferner in Tirol, Le Heron et al., 2021), but are generally rare. It is not thought that these have been recognised in the Pasterze forefield during 'snapshots' of the glacier's retreat. Observations from Skálafellsjökull, Iceland from sondes placed within the subglacial substrate suggest that flutes can form throughout the year, imply continuous formation and moulding of subglacial till, and probably evolve through a combination of erosional and depositional processes (Hart et al., 2018). Elsewhere, anisotropy of magnetic susceptibility (AMS) measurements conducted on fluted till in the forefield of Múlajökull, Iceland, support the idea that till is 'sucked in' to a water filled cavity then progressively expands in the lee of a boulder down glacier (Ives & Iverson, 2019). In the immediate forefield of the Pasterze Glacier, the occurrence of gulleys crosscutting the flutes, dissecting them into fragmentary components, has taken place since 2018 and underscores the rapidity with which evidence for flutes in the proglacial environment is probably to be eradicated in some settings (Rose, 1991). The occurrence of flutes on plateau-like areas (Figure 2A) is thought to be a result of preferential preservation, because the active glacial meltwater channel (see Section 3.4) occupies a lower area to the north. Thus, owing to their elevated position, the flutes have thus far escaped the effects of cannibalisation by meltwater channels. A similar elevated position with respect to the main meltwater channel at the margin of the Gepatsch Glacier (Tirol, Austria) also explains the preservation of flutes at that glacier forefield (Le Heron et al., 2021).

Two observations require explanation, namely (i) the slightly oblique orientation of the flutes with respect to the valley thalweg and (ii) the timing of their formation in the context of ice margin retreat. With regard to the first phenomena, it is inferred that the orientation records an evolution in ice flow direction over time, and may record the local effect of bedrock obstacles. Within the family of subglacial bedforms built from unconsolidated sediment, flutes have been argued to have a distinct origin to larger structures such as drumlins or mega-scale glacial lineations (Ely et al., 2016). Nevertheless, an alternative explanation would be that this part of the ice margin was characterised by heterogeneous flow velocities, for example brought about by the development of flanking folds in the ice (Mayrhofer et al., 2022, explaining the deviation in the orientation of the flutes with respect to overall ice flow direction). Irrespective of the debate surrounding whether flutes represent cavity fill deposits or originate via flow cells (the instability theory; Roberson et al., 2011) they imply sustained flow and thereby a 'healthier' glaciological setting in comparison to the modern ice margin.

3.4 | Ice-marginal assemblage: Description

The ice-marginal fluvial and deltaic assemblage comprises various complex components that can be summarised as (i) an active channel system, (ii) a delta topset, (iii) terraced deposits and (iv) an ice-marginal lake. Collectively, these deposits in (i-iii) share common lithologies, namely gravel and sand in variable proportions.

The active channel system emerges at the present ice margin (Figure 3A) and continues approximately 750 m downtract, before terminating on the delta topset. As of August 2021, this system consists of a shallow (<1 m), narrow (25–50 m wide) channel with several largely submerged 30–50 m long braid bars (Figures 1 and 3A). Flow styles range from subcritical to supercritical, with well-expressed standing waves. Geomorphologically, the active channel system is topographically constrained between the ice margin to the south and terrace deposits to the north. Approximately 400 m from the ice margin, the channel system narrows and follows the course of a small canyon, *ca* 10 m deep, which dissects sands and gravels immediately south of the main valley margin (Figures 1 and 3B). A 2021 panoramic view of the currently inaccessible northern canyon walls reveals its stratigraphic architecture (Figure 3C,D). Orange coloured pebbly sand is organised into low-angle trough cross-strata, expressed in the canyon wall as a series of metre-scale sets. The coarser (gravel-grade) intervals reveal larger (up to 5 m amplitude) foresets. The canyon wall sediments are locally concealed by alluvial cones that extend from a major terrace at the apex of the delta to the present-day river at the bottom. Where equant clasts are present, some of the gravel packages show well-defined imbrication. The sand intervals exhibit

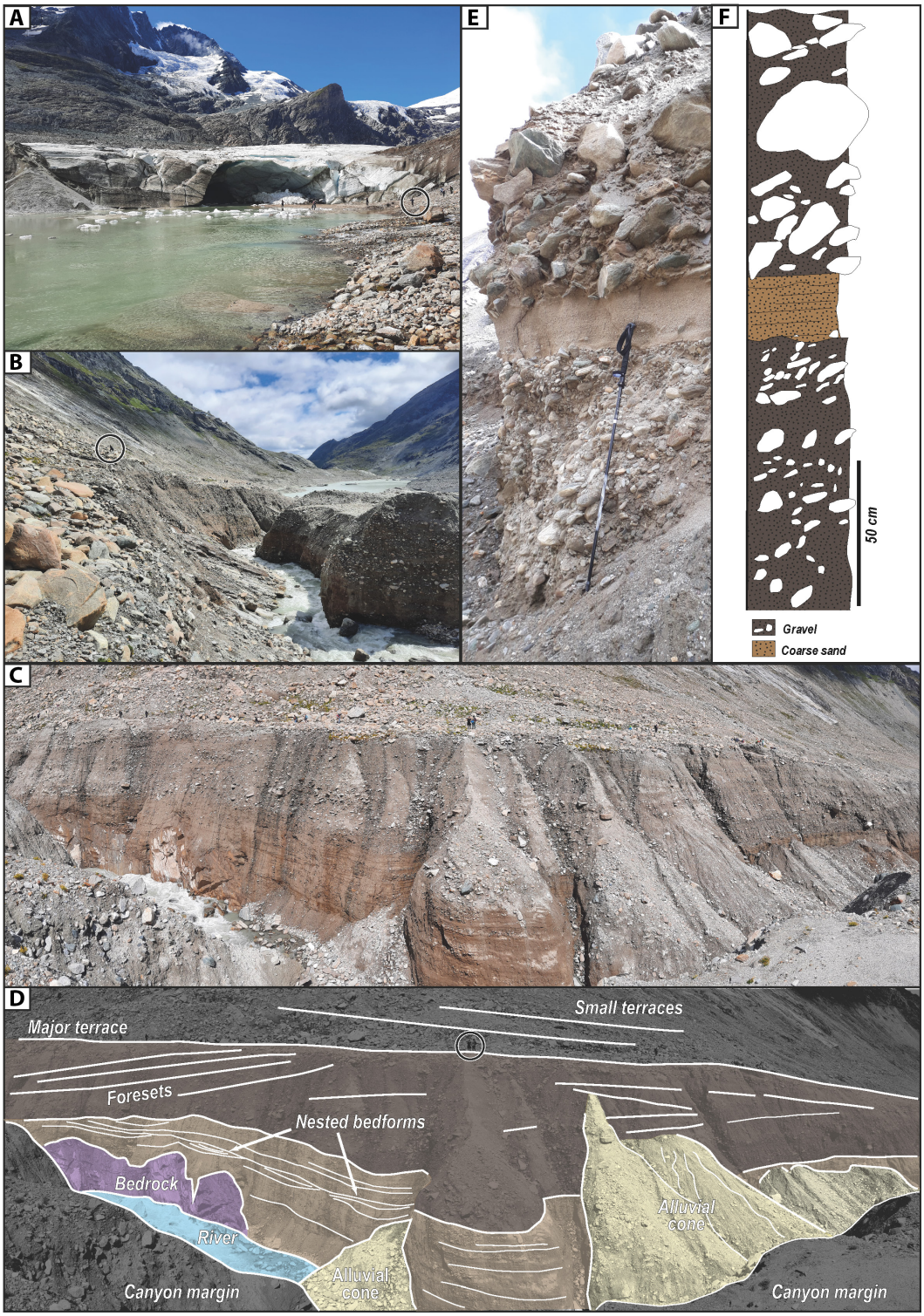

FIGURE 3 The active channel system within the ice-marginal fluvial and deltaic sediment–landform assemblage. (A) View of the ice margin as of August 2021, looking west with a large subglacial conduit in the background emerging as an active channel system (in the foreground). (B) View toward the west in August, 2021 (away from the ice margin) into the narrow canyon and the active channel that feeds the delta topset. (C and D) Panoramic photopanel and interpretation of the northern wall of the small canyon, showing the sedimentary architecture of the proglacial fluvial sediments. (E and F) Photograph and sedimentary log, respectively, of an accessible part of the canyon wall (from July, 2018). Note good evidence of imbrication.

parallel lamination, and isolated small pebbles. A small section of this canyon (Figure 3E) which was then partly ice covered, was logged in 2018 (Figure 3F). Previously, Krainer and Poscher (1992) described stacked planar cross-beds from similar sediments at the 1991 ice margin; in addition to these, the modern ice margin exposes several examples of normally graded sand beds that are either devoid of sedimentary structure or characterised by faint, sub-horizontal lamination.

The delta topset comprises a complex of channels and bars fed by the active channel at the apex and terminating in the ice-marginal lake (Figure 4). In 2018, the ice

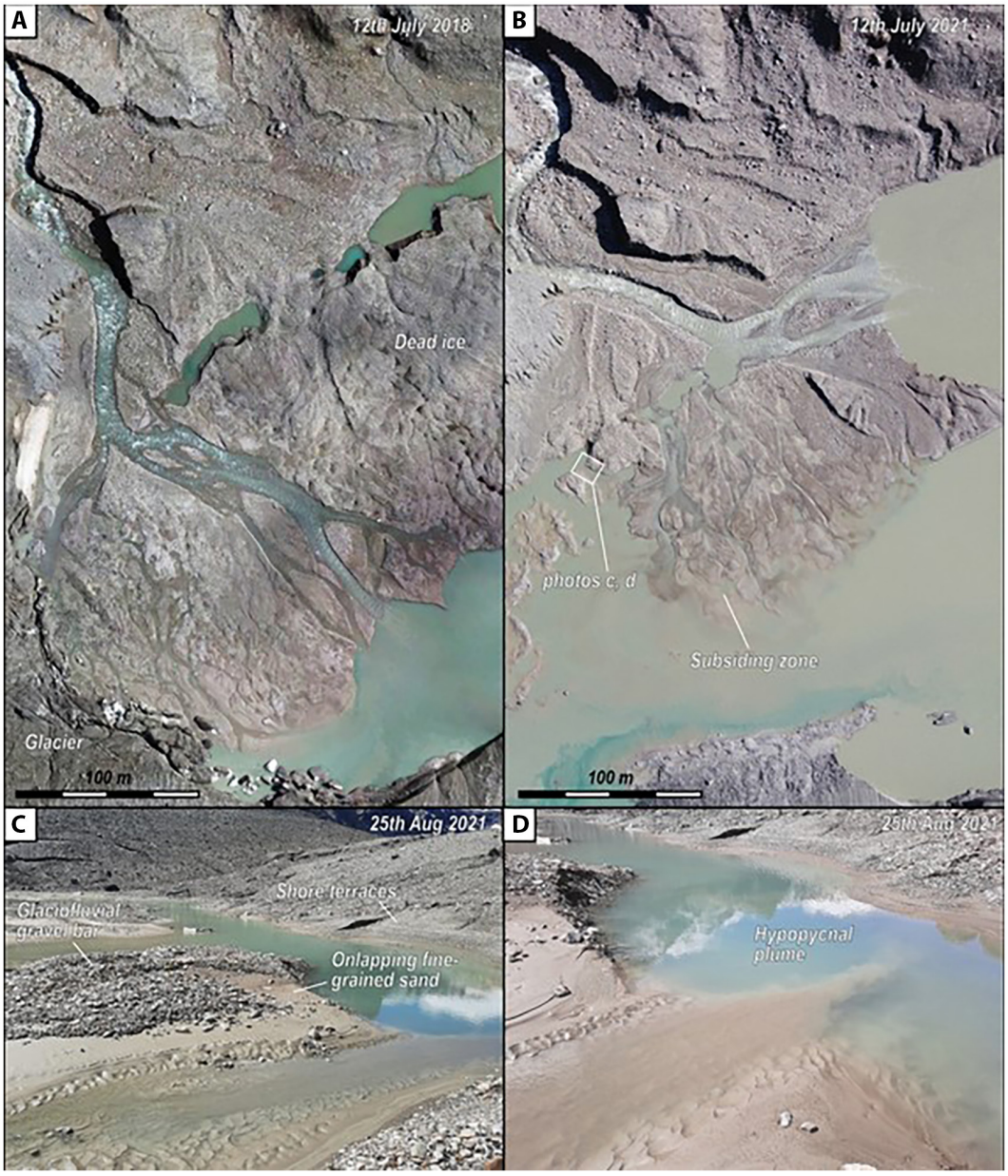

FIGURE 4 The delta topset within the ice-marginal fluvial and deltaic sediment–landform assemblage. (A) Aerial photograph of the topset as of 12 July 2018. Note the occurrence of a major dead ice block to the top right of the image, and a predominantly south-directed family of distributaries with well-developed bars on delta top fringe to the bottom left (south). (B) Aerial photograph of identical area exactly 3 years later on 12 July 2021. Note major switch of distributary channel system to an eastward-directed configuration, draining preferentially into the region that was covered by dead ice in 2018. (C) and (D) are images of the western part of the delta top shoreline, taken on 25 August 2021. The former distributaries (fluvial bars) on the delta topset that were active in 2018 are now nourished by a much less powerful distributary. In both (C) and (D), parallel laminated sands can be seen to onlap the former gravel bars, yet these are now exposed to reveal microterraces (implying base-level fall in this region of the topset). The presence of hypopycnal plumes is surprising given the fact that the distributaries debouch into a lake, but it is suggested that this results from the temperature differences between the (warmer) incoming water and the (ice-cooled) lake.

margin was in contact with the southern corner of the delta topset, and its southern part was fed by a series of distributaries (Figure 4A). By 2021, the drainage pattern is reorganised, so that the topset is fed by one major active distributary channel draining into the northern side of the lake; meanwhile, in the south, a complex network of gravel bars occurs and abandoned channels mark the position of the former distributaries (Figure 4B,C). At ground level, the major active distributary in the north occupies a lower elevation than the abandoned channels and gravel bars to the south of it, from which it is separated by a levee (Figure 4B). Comparison between aerial photographs taken exactly 3 years apart indicates clear-cut channel and bar geomorphology to the south of the topset in 2018 which by 2021 has degraded to poorly defined outlines. The present shoreline of the delta topset locally shows evidence of multiple centimetre-scale, microterraces at the lake shoreline (Figure 4C). These comprise parallel laminated sands which onlap the fluvial gravel bars. As of August 2021, these parallel laminated sands were dissected by small (1 m wide, 15 cm deep) channels, containing lunate current ripples at their margins and highly elongate current ripples to primary current lineations toward the middle of the channel (Figure 4C). The channels have a significant suspended load, as evidenced by the development of hypopycnal plumes at their discharge point into the ice-marginal lake (Figure 4D).

Terraced deposits are best preserved toward the north of the ice margin (Figures 1, 4B and 5A). Here, dozens of staircase-like terraces separated by a few metres are well expressed, and locally dissected by alluvial cones (Figure 1). Compositionally, the terrace deposits comprise gravels, gravelly sands and sands, locally exhibiting the same sedimentary structures observed within the active channel system deposits (namely metre-scale sets of cross-strata in sand, and larger low-angle foresets). Sands are locally well sorted, show subtle evidence for normal grading, and parallel laminations (Figure 5B). The terrace deposits abut against the delta topset to the west, and directly against the ice-marginal lake to the east. The ice-marginal lake periodically contains large icebergs (Figures 1 and 5C), which Kellerer-Pirklbauer et al. (2021) proposed originate from the lake bottom rather than through subaerial calving at the ice margin.

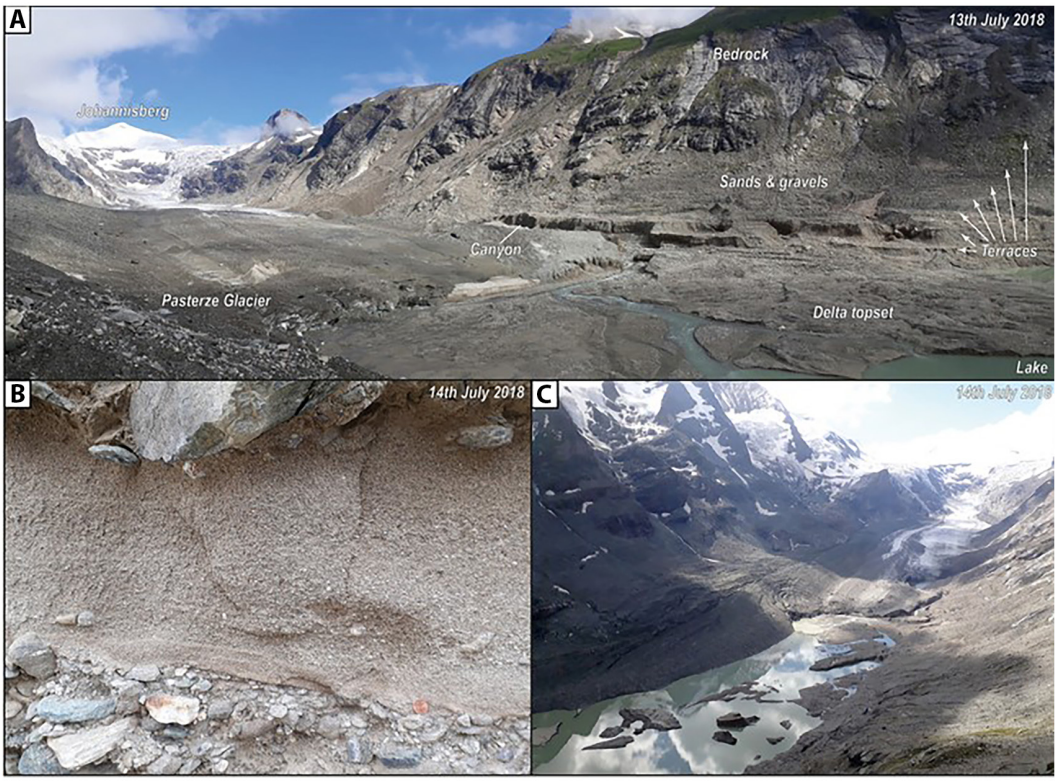

FIGURE 5 Terraced deposits and the ice-marginal lake within the ice-marginal fluvial and deltaic sediment–landform assemblage from July 2018. (A) Overview on the glacier margin, the delta topset, the canyon with the active channel and the clearly expressed terraces constructed of gravel and sand in the background. The terraces are of the order of 1–5 m apart. (B) Example of normally graded, parallel laminated sand sandwiched between two gravel intervals within the terraced deposits. Perspective of the ice-marginal lake and glacier, showing a large number of icebergs. These are sourced from the lake bottom (Kellerer-Pirklbauer et al., 2021).

3.5 | Ice-marginal assemblage: Interpretation

The active channel system records variable yet sustained discharge of meltwater at the transition from the subglacial to the proglacial environment. The alternation of sand and gravel-rich intervals testify to this variability, recognised as the deposits relatively lower and higher discharges respectively. This records the sum of diurnal and seasonal variations, manifested as phases where sand and gravel bedload were dominant. Inaccessibility of the glacier margin in the winter months inhibits study of processes and sediments at that time, but it is tentatively suggested that the orange, cross-bedded sands may record a tendency toward sand-dominated active channels during phases of relatively reduced lower meltwater release. In this interpretation, lower discharge intervals are associated with the formation and migration of sand bars, but gravel bar formation is inhibited owing to the lower transport capacity. During intervals of more significant meltwater release, by contrast, increased discharge led to increased transport capacity, and the evolution of gravel bars, explaining the development of the larger (5 m amplitude) foresets. At peak flow, the meltwater channel is probably to have winnowed and cannibalised the sand-dominated intervals, explaining the clear grain-size dichotomy of gravel and sand in the measured section. Lang et al. (2021) provided a comprehensive review of sedimentary facies associated with supercritical flows in glaciofluvial and glaciodeltaic contexts. The typical sedimentary structures that might indicate catastrophic flows (e.g. climbing dunes, chute and pool structures and other features related to energetic hydraulic jumps; Lang et al., 2021) are lacking from the Pasterze fluvial deposits.

In 1991, before the full development of the proglacial lake, large areas of (then subaerial) sands and gravels were available to study. At that time, Krainer and Poscher (1992) were able to demonstrate, through the presence of sedimentary structures such as stacked climbing ripples and abundant dewatering structures, evidence for sustained sediment supply during sand deposition. Furthermore, decimetre-scale interbeds on the then subaerial sandur surface demonstrated finer intercalations between sand and gravel than it has been possible to show from the 2018 or 2021 ice margins (Krainer & Poscher, 1992, their figure 16). These smaller scale intercalations of finer and coarser debris probably represent short term (diurnal) variations in discharge.

The delta topset records a complex series of processes and products operating at multiple scales. The primary control on delta top geomorphology and sediment distribution is probably to have been avulsion, which is the dominant process in generating the fan-like geometry of distributive sedimentary systems (Weissmann et al., 2010). The high proportion of channel deposits (gravels) in such delta tops naturally leads to high rates of avulsion, a relationship well-documented also in large-scale fluvial-delta systems such as the Rhine-Meuse system (Stouthamer et al., 2011). The appearance of islets toward the south of the delta topset, in tandem with much poorer channel-bar definition in this area is interpreted to result from avulsion-led switch off of the main distributary, cutting off sediment supply, and leading to general delta margin subsidence and compaction. However, the onlap of thinly bedded sands onto 'stranded' gravel bars at the leading edge of the delta top (Figure 4C) testifies to local rejuvenation of minor distributaries. Gradual base-level fall at the leading edge of the delta topset, leading to the generation of microterraces at the lake shoreline, has thus fostered the incision of these sands by the rejuvenated, minor distributaries (Figure 4C). The presence of overflows debouching into the lake (Figure 4C) is an interesting observation, given that this process is typically allied to littoral (marine) systems (Zavala et al., 2021). Indeed, it can be probably explained in terms of the thermal regime of the ice-marginal lake. Given that a substantial part of the glacier snout is in contact with the lake (Figure 1), it has the potential to refrigerate it, and suppress the effects of diurnal warming. Shallow distributaries, meanwhile, transport water that has warmed, enabling them to transport mud debouched into the lake as a plume. With the exception of its termination in a lake, the topset and facies are comparable to those of classic meltwater-dominated end moraine fans described from the Pleistocene record (Krzyszkowski & Zieliński, 2002).

The terraced deposits, characterised by stratigraphically recurrent sands and gravels and few metres to tens of metres above the active channel system, are mostly interpreted as recording earlier phases of fluvial deposition, with one subtle difference to earlier interpretations (Kellerer-Pirklbauer et al., 2021). This difference is that the presence of normally graded, massive to parallel-laminated sands might be more compatible with a turbidite interpretation, similar to those deposited at the margins of classic Quaternary ice-marginal delta systems (Lang et al., 2021; Winsemann et al., 2018). In this context, supported also by the presence of pebbles, the parallel stratified sands also testify to a high energy upper plane bed regime, an interpretation in accord with previous work at the 1991 margin (Krainer & Poscher, 1992). Thus, the terrace deposits are interpreted to contain subtle intercalations of sand deposited in a standing body of water. This may have represented a small lake. The present, well-defined staircase geometry of the terraces (Figure 5A) record kame terraces. These are interpreted to record progressive incision and cannibalisation of ice-marginal sands and gravels, rather

than the development of multiple lateral moraines at progressively lower levels in the valley during glacier snout downwasting. The internal stratigraphy of the terraces, which is exemplified in the small canyon through which the active channel system passes, underscores this interpretation. Therefore, the origin of these sand and gravel deposits through other mechanisms (e.g. as 'Hochsander' fans from supraglacial debris; Kjær et al., 2004, can be ruled out).

Open questions remain over the origin of the small canyon system through which the active channel system passes. Mindful of the above considerations, it is proposed that the canyon is probably to have a hybrid origin, partly recording subglacial incision together with cycles of terrace incision and fluvial sedimentation. The geometry suggests distinct and sustained downcutting through former generations of ice-marginal sediments. The evidence for repeated cannibalisation allows the deposits of the active channel system, the delta topset and the terraced sediments to be viewed as transient deposits rather than long term storages of material, in contrast to the distributive fluvial systems in front of expansive, flat Piedmont glaciers in Iceland (Chandler et al., 2020).

3.6 | Supraglacial assemblage: Description

The supraglacial sediment–landform assemblage (Figure 6) is diverse and comprises at least four separate components. These include (i) angular clast-rich deposits concentrated in broadly ice-flow parallel bands in the ice (Figures 1 and 6A), (ii) large, fan-shaped accumulations of unsorted material on blocks of dead ice (Figure 1), (iii) dirt cones (Figure 6B,C) and (iv) bedded sand and gravel deposits (Figure 6E,F). The characteristics of each are outlined in turn below. First, the angular clast-rich deposits in broadly ice-flow parallel bands show subtle (decimetre-scale) elevation differences with intervening clean (i.e. debris poor) zones on the surface of the glacier. An extreme example of this are 'glacier tables' (Alean et al., 2020) which consist of boulders supported by an ice column.

Dirt cones represent the second component of the supraglacial assemblage. Well-expressed examples of these were studied in July 2018. They comprise well-sorted sands that form a veneer over an ice-cored ridge, in turn mantled by gravel (Figure 6B,C). Sand contains lamination that is parallel with respect to the surface of the steeply dipping ice core beneath. In such occurrences, deposits are typically only a few centimetres thick (where sand is present) or one clast thick (in the case of gravel). Some of these deposits are traversed by supraglacial streams (Figure 6D).

The third component of the supraglacial assemblage comprises major fan-shaped accumulations of debris that are well-developed on the northern glacier margin (Figure 1). Three major, gullied, fan-shaped accumulations, each with an area exceeding 20,000 m^2, are mapped. Well-defined apices of these accumulations occur, and material downlaps onto the surface of the glacier, giving the structures the appearance of a series of alluvial fans. The easternmost of these comprises a cauldron structure in its upper reaches, and could be accessed immediately north of the summer 2021 ice margin. The material comprises sand to boulder grade, unsorted and often ice-cored sediment, mantling and flanking large dead ice blocks at the glacier margin. Lithologically, a spectrum of poorly-sorted sandy gravels to diamictons are recognised.

The fourth component of the supraglacial assemblage, exemplified by deposits at the July/August 2021 margin, consists of well-bedded sand and gravel accumulations of up to several metres thick (Figure 6E). Outcrops occur as both approximately circular accumulations on dead ice blocks, as well as approximately ice-margin parallel ridges. Stratified sandy gravels and gravelly sands form decimetre-scale layering in which individual strata contain well-sorted sediments (Figures 1 and 2A). Imbrication is observed, and decimetre-scale cross stratification is also well expressed. The boundaries between 'beds' are not always well defined, some are gradational, and examples of both upward-coarsening and upward-fining are observed.

3.7 | Supraglacial assemblage: Interpretation

Individual components of the supraglacial assemblage are interpreted to have differing origins and are accordingly considered in turn below. First, the angular clast-rich deposits concentrated in broadly ice-flow parallel bands in the ice are interpreted to have originated as rockfall-generated debris. This interpretation is consistent with previous work that focussed specifically on these pathways of sediment production (Kellerer-Pirklbauer, 2008), explaining the angularity of material which is attributed to short transport distance.

Interpreting the second component of the supraglacial assemblage, namely the dirt cones, is somewhat more complex, yet analogues can be found from other temperate glaciers. Glasser et al. (2003) described debris-charged ridges emerging from steeply dipping fractures near the snout of Storglaciären in Sweden. Similarly, at the Haut Glacier d'Arolla in Switzerland, a close relationship with reactivated crevasse traces and supraglacial material forming medial moraines and so-called 'dirt cones' was interpreted by Goodsell et al. (2005) to record the emergence

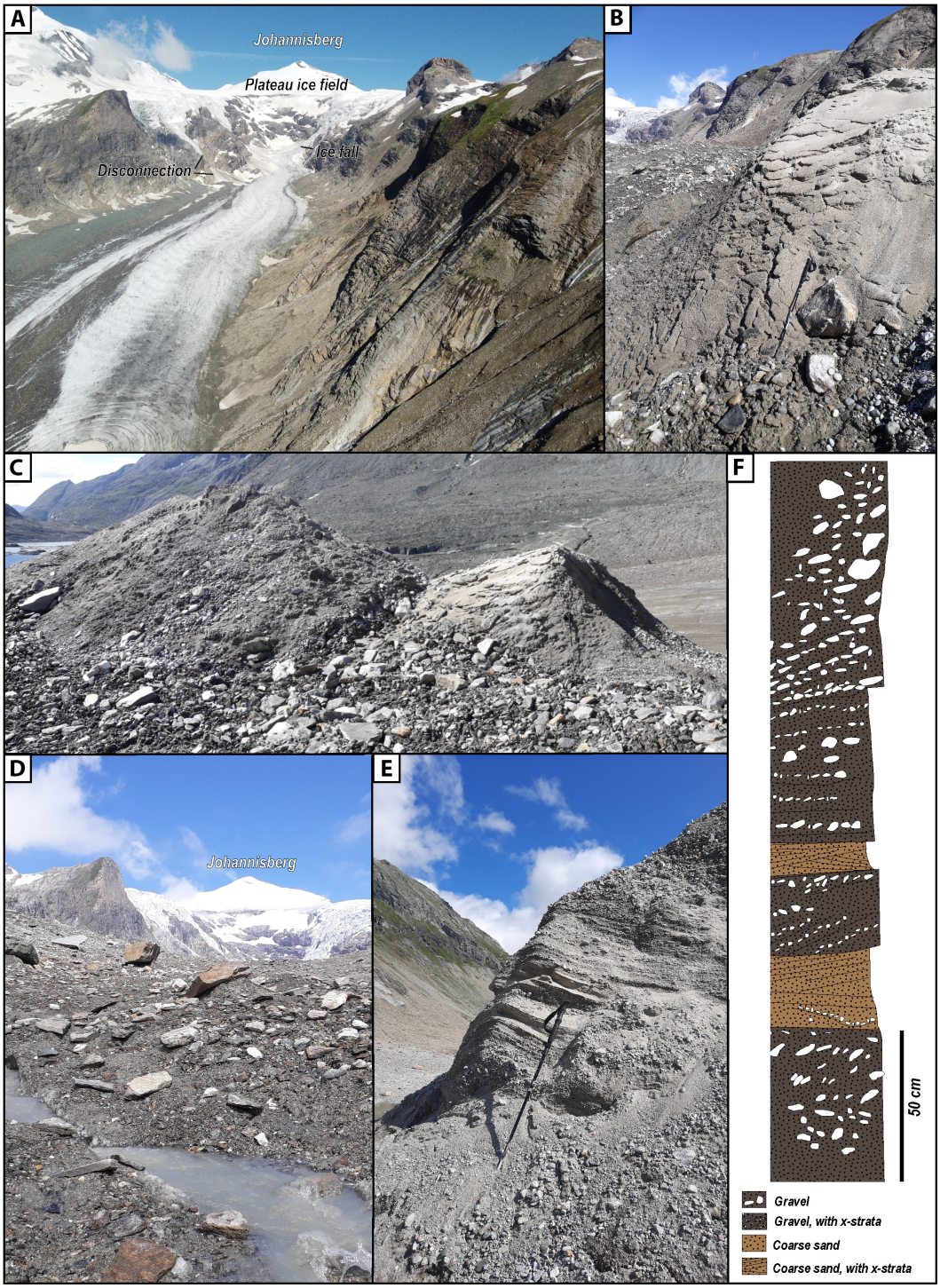

FIGURE 6 (A) Aerial photograph looking west showing the relationship between the Pasterze Glacier and its surroundings (July 2021). The main field of view lies beyond that mapped in Figure 1, with the exception of the 'cauldron structure' and snow-covered moulin seen in the bottom of the image. In the midground, the surface of the glacier shows an abundance of supraglacial debris, plus ogives and foliations mapped in Figure 1. In the background, an ice fall still nourishes the glacier, but otherwise there are disconnections between the plateau icefield and the Pasterze Glacier on the southern valley side. Photographs (B) to (E) show different examples of deposits now found in a supraglacial position. (B) and (C) Dirt cones. These are characterised by a thin veneer of stratified sand lying directly on a convex-up body of ice, passing laterally into gravel (photograph July 2018). (D) A small supraglacial basin, consisting chiefly of supraglacial debris (Kellerer-Pirklbauer, 2008), in turn dissected by a meltwater stream (photo July 2018). (E) Well-preserved intercalated gravels and sands on top of dead ice in front of the 2021 margin (photograph August 2021). (F) Sedimentary log of the section shown in photograph (E).

of debris layers along crevasses. Such a tentative interpretation would be compatible with the strike of the ice-flow normal foliation in the Pasterze Glacier (Figure 1), yet remains to be fully demonstrated. In contrast, the thin sand and gravel layers mantling ice-cored ridges are interpreted as supraglacial stream deposits sitting in inverted relief as a result of locally protecting the underlying ice from ablation. These probably represent deposition in crevasses. Note, however, that sand lamination tracking the position of the underlying ice body on the Pasterze also point to post-deposition modification resulting from the ice melting process, and thus a combination of these two processes is probably.

Third, the major fan-shaped accumulations of debris are considered to have a hybrid origin consisting of in situ deposition of subglacial and englacial material through downwasting of the glacier (i.e. in situ meltout/glacier surface lowering). In this process, the incipient development of a lateral moraine combined with material fluxed onto the glacier surface through gravitational instability from the steep bedrock slopes. They are therefore best interpreted as rock avalanche moraines (Schomacker & Benediktsson, 2018). Rock avalanche sediments deposited in a non-glacial, upland environment typically include a zoned structure, with shear zones and fragmented facies, 'jigsaw facies', and a very blocky carapace that should allow them to be recognised in the field (Dufresne et al., 2016). These criteria are, unfortunately, of little use in a supraglacial context where downwasting of underlying dead ice is expected to destroy these textures, and leads to great difficulty in distinguishing them from moraines in the postglacial landscape (Hewitt, 1999). The resulting debris carapace has thus protected large swathes of underlying ice from ablation at the northern margin of the valley. The ultimate fate of these, if not fully destabilised by downwasting, may be to produce large lateral moraines (Lukas et al., 2012).

Finally, the well-bedded sand and gravel deposits are interpreted as the deposits of either supraglacial river deposition, analogous to sediments found in extant meltwater streams on the glacier surface (Figure 6D), or those of an esker. The lithologies together with the predominance of cross-strata in both the gravel and sand fraction bear close resemblance to the facies associated with both active channel and terraced deposits in the ice-marginal assemblage. Evidence for clast imbrication in the gravelly facies (Figure 6F) testifies to the role of meltwater here. The sole distinguishing factor is that they rest on a (dead-ice) substratum. Therefore, the intercalation of sands and gravels probably record alternating subcritical and supercritical flow deposits in the fluvial environment, with the upward-coarsening and upward-fining motifs consistent with highly variable discharge conditions (Lang et al., 2021; Winsemann et al., 2018). It is proposed here that the sand and gravel accumulations record an inverted topography whereby an extensive and several metre-deep supraglacial river became filled with coarse clastic detritus. This protected the underlying ice from ablation, explaining the remnants of these deposits upon small hills at the ice margin.

4 | DISCUSSION

Multiple lines of evidence suggest that the Pasterze Glacier can be characterised as a dying glacier. This evidence includes (i) disconnections of two of the three ice falls feeding the glacier from the ice field, (ii) rapid surface elevation loss of the snout as measured using LiDAR in previous studies (Avian et al., 2018), (iii) flow stagnation (Mayrhofer et al., 2022) and (iv) development of extensive lakes on top of the glacier tongue that could easily be mistaken for a proglacial lake (Kellerer-Pirklbauer et al., 2021). Accordingly, it is no exaggeration to refer to the sediment–landform assemblage of the present day Pasterze as its sedimentary deathmask. This is especially apposite given the evidence, from emerging icebergs at the bottom of the proglacial lake (Kellerer-Pirklbauer et al., 2021), that a significant portion of the 'proglacial' sedimentary system actually represents supraglacial sedimentation. This being the case, the ice-marginal delta system described herein may represent a supraglacial system, at least in part, rather than a classic regressive delta observed in many ice-marginal areas of the Quaternary record (Winsemann et al., 2018). In their review, Schomacker and Benediktsson (2018) considered six main processes that cause supraglacial sediment to accumulate. These were (i) rockfalls and avalanches, (ii) thrusting/squeezing of subglacial material, (iii) meltout of englacial debris bands, (iv) deposition from meltwater on the surface, (v) deposition of airborne dust from multiple sources and (vi) deposition of extraterrestrial (space) material. Unless process (iv) in the preceding list is interpreted very broadly, it is clear that process models for supraglacial debris do not entertain the possibility of hybrid supraglacial–proglacial lakes.

The rather sunken appearance of the southern portion of the delta (Figures 1 and 3B) is consistent with deposition of foresets and topsets on the buried surface of the glacier, rather than buildout onto a previously deposited sediment. The poorly defined channel domains in this region in 2021 compared to 2018 (c.f. Figure 3A,B) may thus imply rapid subsidence caused by melting of buried ice at the lake bed, as well as compaction driven-subsidence of the delta top as a result of avulsion of channels away from this region. In Iceland, Kjær and Krüger (2001) showed that the process of 'de-icing' of dead ice moraine may result in the development of kettle holes and the general

slumping of supraglacial debris. In a similar way, it is predicted that the delta architecture will become modified, potentially through slumps into the lake, as the lake-bed ice continues to melt. The spatial relationships between the small canyon system and the sediments into which it incises hints at processes of forced incision at the ice front (Winsemann et al., 2018). This is because the interbedded sands and gravels that comprise the walls of the canyon are identical to those that are observed in the modern river, indicating significant incision of approximately 10 m and cannibalisation of earlier-deposited ice-marginal deposits.

Using digital elevation models of difference collected by a fixed wing uncrewed aerial vehicle (UAV) collected 51 days apart in the 2016 meltwater season, Seier et al. (2017) showed that the Pasterze margin experienced in the range of 1–3 m of elevation loss. With this remarkable figure in mind, as of 2021, it is now questionable whether the Pasterze Glacier is any more than a large block of dead ice at the margin. In 2019, two connections to a small plateau icefield remained, and no connection to tributary glaciers remained (Avian et al., 2020). In 2021, it was observed that one of the ice falls immediately to the north of Großglockner mountain had become disconnected, and thus the glacier is nourished only by a very small icefall to the extreme west of the glacier basin (Figure 6A). Classically, the Pasterze would belong to the temperate, high relief glacier type (Hambrey & Glasser, 2012), consistent with the significant input from rockfalls and the abundance of supraglacial debris. Nevertheless, given the transition of the Pasterze to a large dead ice block, a specific facies model for a dying glacier should be established, although not all dying glaciers are necessarily so debris-charged as the Pasterze. This contribution has shown how specific elements of the 2021 ice-marginal system, notably the presence of hybrid supraglacial/proglacial deltas, are somewhat unusual, and whose spatial development is not typically accounted for either in facies models of supraglacial environments (Schomacker & Benediktsson, 2018).

Integrating the interpretations of the subglacial assemblage, the ice-marginal fluvial and deltaic assemblage and the supraglacial assemblage, a schematic model is presented for the present day Pasterze Glacier, characterised as a dying glacier landsystem (Figure 7). This landsystem is distinguished from established glaciated valley landsystems (Benn et al., 2005) in the following important aspects. First, lateral moraines do not actively develop: instead, large, fan-like bodies of supraglacial material develop on dead ice at the margins in concert with rockfall material. Second, development of large volumes of meltwater floods

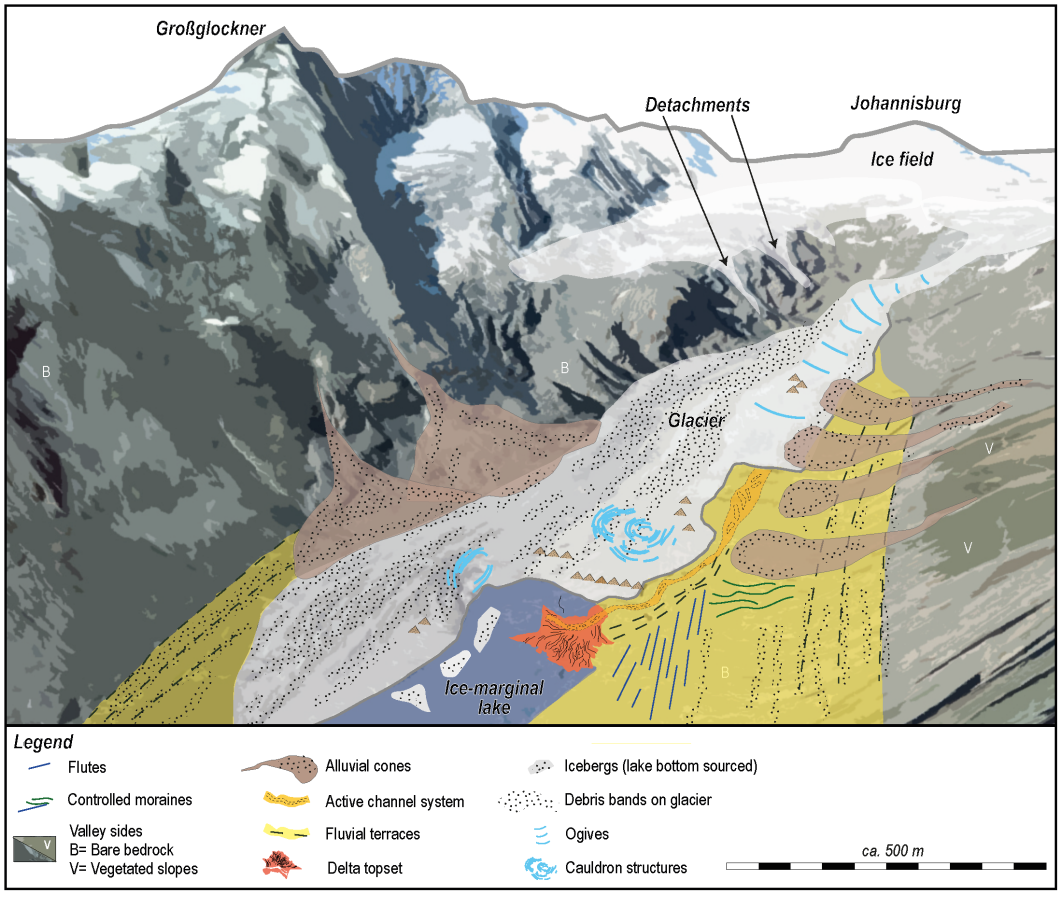

FIGURE 7 A simple model for a dying glacier landsystem, as exemplified by the modern day Pasterze Glacier, Austria.

low-lying dead ice at the margin and deltas build out into an ice-floored lake. Third, the role of meltwater incision and cannibalisation is accentuated by comparison to glaciers associated with a 'healthy' glaciated valley landsystem, leading to ever deeper canyonisation through previously deposited sands and gravels. Fourth, connections between the nourishing plateau ice field and the trunk glacier are weakened to severed. The latter results in disconnections, an increasingly widely recognised phenomenon that is recognised as vital for the long term stability of alpine and maritime ice masses (Laute & Beylich, 2021).

5 | CONCLUSIONS

- A hybrid glaciological–geomorphological–sedimentological map of the margin of the Pasterze Glacier reveals a snapshot of the sedimentary environments and facies distributions at its margin. Three sediment–landform assemblages are recognised: (i) a subglacial assemblage, (ii) an ice-marginal fluvial and deltaic assemblage and (iii) a supraglacial assemblage.
- The subglacial assemblage includes evidence for a flute field, mapped on aerial photography and observed to occur on a slightly elevated plateau. The flutes probably survived cannibalisation at the ice margin by the diversion of subglacial meltwaters into low-lying areas either side of the plateau.
- The ice-marginal fluvial and deltaic assemblage consists of alternating gravel and sand deposits feeding an ice-marginal delta. Significant cannibalisation and downward incision has occurred in the fluvial (topset) part of the delta to produce a *ca* 10 m deep canyon. Given the recognition that the ice-marginal lake into which the delta builds at least partly represents a supraglacial lake on part of the glacier snout, avulsion of distributaries on the delta top as well as subsidence patterns are also probably driven by ablation and downwasting on the ice.
- The supraglacial assemblage includes typical rockfall deposits but also well-preserved, well- differentiated sand and gravels. Thin sand and gravel deposits are identified as possible former (exhumed) englacial deposits; thicker interbedded sands and gravels are identified as the deposits of variable energy fluvial discharge on the glacier surface.
- It is proposed that the sediment–landform assemblages at the Pasterze Glacier allow characterisation of a dying glacier landsystem which is distinct from previous models of glaciated valleys.

ACKNOWLEDGEMENTS

We are very grateful to the perceptive and extremely valuable reviews of Clare Boston and Anonymous, whose comments definitely led to an improvement in the finished manuscript. To this end, we are grateful to Elias Semankassou for taking on the handling of the manuscript and for communicating clearly what was required. Finally, we wish to thank our institution, the University of Vienna, for funding our sedimentological research in the Pasterze area.

DATA AVAILABILITY STATEMENT

n/a.

ORCID

Daniel Paul Le Heron https://orcid.org/0000-0002-7213-5874

REFERENCES

Alean, J., Schwendener, L. & Zemp, M. (2020) Migrating boulders on the surface of Alpine valley glaciers. *Geografiska Annaler, Series A: Physical Geography*, *103*, 151–166. https://doi.org/10.1080/04353676.2020.1850064

Avian, M., Bauer, C., Schlögl, M., Widhalm, B., Gutjahr, K.-H., Paster, M., Hauer, C., Frießenbichler, M., Neureiter, A., Weyss, G., Flödl, P., Seier, G. & Sulzer, W. (2020) The status of earth observation techniques in monitoring high mountain environments at the example of Pasterze Glacier, Austria: Data, methods, accuracies, processes, and scales. *Remote Sensing*, *12*(8), 1251. https://doi.org/10.3390/rs12081251

Avian, M., Kellerer-Pirklbauer, A. & Lieb, G.K. (2018) Geomorphic consequences of rapid deglaciation at Pasterze Glacier, Hohe Tauern Range, Austria, between 2010 and 2013 based on repeated terrestrial laser scanning data. *Geomorphology*, *310*, 1–14. https://doi.org/10.1016/j.geomorph.2018.02.003

Benn, D.I., Kirkbride, M.P., Owen, L.A. & Brazier, V. (2005) Glaciated Valley Landsystems. In: Evans, D.J.A. (Ed.) *Glacial landsystems*. London: Hodder Arnold, pp. 372–405.

Chandler, B.M.P., Evans, D.J.A., Chandler, S.J.P., Ewertowski, M.W., Lovell, H., Roberts, D.H., Schaefer, M. & Tomczyk, A.M. (2020) The glacial landsystem of Fjallsjökull, Iceland: Spatial and temporal evolution of process-form regimes at an active temperate glacier. *Geomorphology*, *361*, 107192. https://doi.org/10.1016/j.geomorph.2020.107192

Chandler, B.M.P., Lovell, H., Boston, C.M., Lukas, S., Barr, I.D., Benediktsson, Í.Ö., Benn, D.I., Clark, C.D., Darvill, C.M., Evans, D.J.A., Ewertowski, M.W., Loibl, D., Margold, M., Otto, J.C., Roberts, D.H., Stokes, C.R., Storrar, R.D. & Stroeven, A.P. (2018) Glacial geomorphological mapping: A review of approaches and frameworks for best practice. *Earth-Science Reviews*, *185*, 806–846. https://doi.org/10.1016/j.earscirev.2018.07.015

Cornelius, H.P. & Clar, E. (1935) Geologische Karte des Glocknergebietes. *Wien, Alpenverein und Geologische Bundesanstalt*, *1*, 25000.

Dufresne, A., Bösmeier, A. & Prager, C. (2016) Sedimentology of rock avalanche deposits—case study and review. *Earth Science Reviews*, *163*, 234–259. https://doi.org/10.1016/j.earscirev.2016.10.002

Ely, J.C., Clark, C.D., Spagnolo, M., Stokes, C.R., Greenwood, S.L., Hughes, A.L.C., Dunlop, P. & Hess, D. (2016) Do subglacial bedforms comprise a size and shape continuum? *Geomorphology*, *257*, 108–119. https://doi.org/10.1016/j.geomorph.2016.01.001

Glasser, N.F., Hambrey, M.J., Etienne, J.L., Jansson, P. & Pettersson, R. (2003) The origin and significance of debris-charged ridges at the surface of Storglaciären, northern Sweden. *Geografiska Annaler, Series A: Physical Geography*, *85*, 127–147. https://doi.org/10.1111/1468-0459.00194

Goodsell, B., Hambrey, M.J. & Glasser, N.F. (2005) Debris transport in a temperate valley glacier: Haut Glacier d'Arolla, Valais, Switzerland. *Journal of Glaciology*, *51*, 139–146.

Hambrey, M.J. & Glasser, N.F. (2012) Discriminating glacier thermal and dynamic regimes in the sedimentary record. *Sedimentary Geology*, *251–252*, 1–33.

Hart, J.K., Clayton, A.I., Martinez, K. & Robson, B.A. (2018) Erosional and depositional subglacial streamlining processes at Skálafellsjökull, Iceland: an analogue for a new bedform continuum model. *GFF*, *140*, 153–169. https://doi.org/10.1080/11035897.2018.1477830

Herbst, P. & Neubauer, F. (2000) The Pasterze glacier, Austria: an analogue of an extensional allochthon. *Geological Society, London, Special Publications*, *176*, 159–168. https://doi.org/10.1144/GSL.SP.2000.176.01.12

Hewitt, K. (1999) Quaternary moraines vs catastrophic rock avalanches in the Karakoram Himalaya, Northern Pakistan. *Quaternary Research*, *51*, 220–237. https://doi.org/10.1006/qres.1999.2033.

Hugonnet, R., McNabb, R., Berthier, E., Menouros, B., Nuthm, C., Girod, L., Farinotti, D., Huss, D., Dussaillant, I., Brun, F. & Kääb, A. (2021) Accelerated global glacier mass loss in the early twenty-firstcentury. *Nature*, *592*, 726–731.

Immerzeel, W.W., Lutz, A.F., Andrade, M., Bahl, A., Biemans, H., Bolch, T., Hyde, S., Brumby, S., Davies, B.J., Elmore, A.C., Emmer, A., Feng, M., Fernández, A., Haritashya, U., Kargel, J.S., Koppes, M., Kraaijenbrink, P.D.A., Kulkarni, A. v., Mayewski, P.A., Nepal, S., Pacheco, P., Painter, T.H., Pellicciotti, F., Rajaram, H., Rupper, S., Sinisalo, A., Shrestha, A.B., Viviroli, D., Wada, Y., Xiao, C., Yao, T., & Baillie, J.E.M., 2020. Importance and vulnerability of the world's water towers. *Nature 577*, 364–369. https://doi.org/10.1038/s41586-019-1822-y

Ives, L.R.W. & Iverson, N.R. (2019) Genesis of glacial flutes inferred from observations at Múlajökull, Iceland. *Geology*, *47*(5), 387–390. https://doi.org/10.1130/G45714.1

Kellerer-Pirklbauer, A. (2008) The supraglacial debris system at the Pasterze Glacier, Austria: Spatial distribution, characteristics and transport of debris. *Zeitschrift für Geomorphologie*, *52*, 3–25. https://doi.org/10.1127/0372-8854/2008/0052S1-0003

Kellerer-Pirklbauer, A., Avian, M., Benn, D.I., Bernsteiner, F., Krisch, P. & Ziesler, C. (2021) Buoyant calving and ice-contact lake evolution at Pasterze Glacier (Austria) in the period 1998-2019. *The Cryosphere*, *15*, 1237–1258. https://doi.org/10.5194/tc-15-1237-2021

Kellerer-Pirklbauer, A. & Kulmer, B. (2019) The evolution of brittle and ductile structures at the surface of a partly debris-covered, rapidly thinning and slowly moving glacier in 1998–2012 (Pasterze Glacier, Austria). *Earth Surface Processes and Landforms*, *44*, 1034–1049. https://doi.org/10.1002/esp.4552

Kjær, K.H. & Krüger, J. (2001) The final phase of dead-ice moraine development: processes and sediment architecture, Kötlujökull, Iceland. *Sedimentology*, *48*, 935–952. https://doi.org/10.1046/j.1365-3091.2001.00402.x

Kjær, K.H., Sultan, L., Krüger, J. & Schomacker, A. (2004) Architecture and sedimentation of outwash fans in front of the Mýrdalsjökull ice cap, Iceland. *Sedimentary Geology*, *172*, 139–163. https://www.doi.org/10.1016/j.sedgeo.2004.08.002

Krainer, K. & Poscher, G. (1992) Sedimentologische Beobachtungen im Glet-schervorfeld der Pasterze (Glocknergruppe, Hohe Tauern). Carinthia II *182*, 317–343.

Kronig, O., Ivy-Ochs, S., Hajdas, I., Christl, M., Wirsig, C. & Schlüchter, C. (2018) Holocene evolution of the Triftje- and the Oberseegletscher (Swiss Alps) constrained with ^{10}Be exposure and radiocarbon dating. *Swiss Journal of Geosciences*, *111*, 117–131.

Krzyszkowski, D. & Zieliński, T. (2002) The Pleistocene end moraine fans: controls on their sedimentation and location. *Sedimentary Geology*, *149*, 73–92.

Lagally, M. (1932) Die Bewegung des "toten Eises" an der Pasterze. In: *Z.f. Gletscherkunde XX (Finsterwalder-Festschrift)*. Vienna: Brückner, pp. 215–221.

Lang, J., Le Heron, D.P., Van den Berg, J.H. & Winsemann, J. (2021) Bedforms and sedimentary structures related to supercritical flows in glacigenic settings. *Sedimentology*, *68*, 1539–1579. https://doi.org/10.1111/sed.12776

Laute, K. & Beylich, A.A. (2021) Recent glacier changes and formation of new proglacial lakes at the Jostedalsbreen ice cap in southwest Norway. In: Beylich, A.A. (Ed.) *Landscapes and landforms of Norway*. World Geomorphological Landscapes. Cham, Switzerland: Springer, pp. 71–95. https://doi.org/10.1007/978-3-030-52563-7_4

Le Heron, D.P., Kettler, C., Davies, B.J., Scharfenberg, L., Eder, L., Ketterman, M., Giesmeier, G.E., Quinn, R., Chen, X., Vandyk, T. & Busfield, M.E. (2021) Rapid geomorphological and sedimentological changes at a modern Alpine ice margin: lessons from the Gepatsch Glacier, Tirol, Austria. *Journal of the Geological Society of London*, *179*. https://doi.org/10.1144/jgs2021-052

Le Heron, D.P., Vandyk, T.M., Hongwei, K., Liu, Y., Chen, X., Wang, Y., Yang, Z., Scharfenberg, L., Davies, B. & Shields, G. (2019) Bird's-eye view of an Ediacaran subglacial landscape. *Geology*, *47*, 705–709. https://doi.org/10.1130/G46285.1

Lieb, G.K. (2004) Die Pasterze als Beispiel eines schwindenden Gletschers. In: Zängl, W. & Hamberger, S. (Eds.) *Gletscher im Treibhaus. Eine fotografische Zeitreise in die alpine Eiswelt*. Steinfurt: Tecklenborg Verlag, pp. 216–219.

Lukas, S., Graf, A., Coray, S. & Schlüchter, C. (2012) Genesis, stability and preservation potential of large lateral moraines of Alpine valley glaciers e towards a unifying theory based on Findelengletscher, Switzerland. *Quaternary Science Reviews*, *38*, 27–48.

Mayrhofer, F., Schöpfer, M.P.J., Adamuszek, M., Dabrowski, M. & Grasemann, B. (2022) Transtensional flanking structures. *Journal of Structural Geology*, *161*, 104659. https://doi.org/10.1016/j.jsg.2022.104659

Paschinger, H. (1953) 5 Jahre Pasterzenmessungen 1947-1951. Carinthia II 142/62, 7-15.

Patzelt, G. & Slupetzky, H. (1970) Die Vertikalkomponente der Gletscherbewegung auf der Pasterze 1968-69 und ihr Einfluss auf die Berechnung der Massenbilanz. *Zeitschrift für Gletscherkunde und Glazialgeologie*, *6*, 199–227.

Roberson, S., Hubbard, B., Coulson, H.R. & Boomer, I. (2011) Physical properties and formation of flutes at a polythermal valley glacier: Midre Lovénbreen, Svalbard. *Geografiska Annaler, Series A: Physical Geography*, *93*, 71–88. https://doi.org/10.1111/j.1468-0459.2011.00420.x

Rose, J. (1991) Subaerial modification of glacier bedforms immediately following ice wastage. *Norsk Geografisk Tidsskrift*, *45*, 143–153. https://doi.org/10.1080/00291959108552267

Schomacker, A. & Benediktsson, Í.Ö. (2018) Supraglacial environments. In: *Past glacial environments*. Amsterdam: Elsevier.

Seeland, M. (1883) Studien am Pasterzengletscher IV. *Zeitschrift des Deutschen und Österreichischen Alpenvereins*, *14*, 93–97.

Seier, G., Kellerer-Pirklbauer, A., Wecht, M., Hirschmann, S., Kaufmann, V., Lieb, G.K. & Sulzer, W. (2017) UAS-based change detection of the glacial and proglacial transition zone at Pasterze Glacier, Austria. *Remote Sensing*, *9*. https://doi.org/10.3390/rs9060549

Stouthamer, E., Cohen, K.M., & Gouw, M.J.P., 2011. Avulsion and its implications for fluvial-deltaic architecture: insights from the Holocene Rhine-Meuse Delta: From: River to rock record the preservation of fluvial sediments and their subsequent interpretation. *SEPM Special Publication*, *97*, 215–231.

Veh, G., Korup, O. & Walz, A. (2020) Hazard from Himalayan glacier lake outburst floods. *Proceedings of the National Academy of Sciences*, *117*, 907–912. https://doi.org/10.1073/pnas.1914898117

Wakonigg, H. (1993) Nachmessungen an der Pasterze (Glocknergruppe) von 1971 bis 1990. Z. f. Gletscherkunde und Glazialgeologie 27/28 (1991/92), 191–205.

Wakonigg, H. & Lieb, G.K. (1996) Die Pasterze und ihre Erforschung im Rahmen der Gletschermessungen. In: *Wissenschaft im Nationalpark Hohe Tauern Kärnten*. Großkirchheim: Kärntner Nationalpark-Schriften, Vol. *8*, pp. 99–115.

Weissmann, G.S., Hartley, A.J., Nichols, G.J., Scuderi, L.A., Olson, M., Buehler, H. & Banteah, R. (2010) Fluvial form in modern continental sedimentary basins: Distributive fluvial systems. *Geology*, *38*, 39–42. https://doi.org/10.1130/G30242.1

Winsemann, J., Lang, L., Polom, U., Loewer, M., Igel, J., Pollok, L. & Brandes, C. (2018) Ice-marginal forced regressive deltas in glacial lake basins: geomorphology, facies variability and large-scale depositional architecture. *Boreas*, *47*, 973–1002. https://doi.org/10.1111/bor.12317

Zavala, C., Arcuri, M., Di Meglio, M., Zorzano, A., Otharán, G., Irastorza, A. & Torresi, A. (2021) Deltas: a new classification expanding Bates's concepts. *Journal of Palaeogeography*, *10*, 1–15. https://doi.org/10.1186/s42501-021-00098-w

Zekollari, H., Huss, M. & Farinotti, D. (2019) Modelling the future evolution of glaciers in the European Alps under the EURO-CORDEX RCM ensemble. *The Cryosphere*, *13*, 1125–1146. https://doi.org/10.5194/tc-13-1125-2019

How to cite this article: Le Heron, D.P., Kettler, C., Wawra, A., Schöpfer, M. & Grasemann, B. (2022) The sedimentological death mask of a dying glacier. *The Depositional Record*, *8*, 992–1007. https://doi.org/10.1002/dep2.205